ChemComm

FEATURE ARTICLE

View Article Online
View Journal | View Issue

Cite this: *Chem. Commun.*, 2015, **51**, 624

Tailoring the assembly, interfaces, and porosity of nanostructures toward enhanced catalytic activity

Thanh-Dinh Nguyen,*[a] Cao-Thang Dinh[b] and Trong-On Do*[b]

The evolution of nanotechnology has inspired materials scientists to invent nanostructures with achievements in numerous practical applications, particularly in catalysis. The great advancements typically involve flexible control over the unique properties of the nanomaterial through tuning their structural geometries and components. In this Feature Article, we present the recent progress of our recent research and that of other groups in tailoring the assembly, interfaces, and porosity of diverse inorganic nanostructures. The enhanced catalytic properties of the engineered nanostructures are discussed in relation to photocatalysis, with special emphasis on solar energy conversion, including water splitting, CO_2 reduction, and organic photodecomposition. Considering their attributes of superior catalytic performance and long-term durability, the development of economical, active nanocatalysts opens up practical opportunities for endeavours in sustainable energy conversion and other applied fields. This review is expected to introduce readers to the general principles of engineering the nanostructured features of the inorganic nanomaterials capable of improving solar photocatalytic efficiency.

Received 24th July 2014,
Accepted 19th September 2014

DOI: 10.1039/c4cc05741d

www.rsc.org/chemcomm

Introduction

Chemical methods for growing nanocrystals in solution have achieved significant progress in tuning the structural geometry and components of nanomaterials.[1] The assembly, interfaces, and porosity of the nanostructure are considered as crucial features that can be engineered to affect the properties of the material.[2,3] Thanks to the evolution of nanotechnology allowing mastery in the synthesis of nanostructured features, exquisitely uniform particles that behave like elementary units can be used to build nanoarchitectures for studies on interfacial chemistry.[4] An important topic in materials science is the development of nanostructured catalysts with improved activity. Such nanostructures with tailored geometries are crucial components of many industrially relevant heterogeneous catalysts.[5]

Nanostructured catalysts play an important role in tackling the environmental and energy issues.[6] Since heterocatalytic reactions occur at a catalyst's surfaces, tailoring the geometry of catalysts to expose active phases[2] and amplify reactant

Thanh-Dinh Nguyen

Thanh-Dinh Nguyen studied chemical engineering at Laval University under the guidance of Prof. Trong-On Do, where he received his PhD in 2011. After graduation, he joined Prof. MacLachlan's lab at The University of British Columbia as an NSERC Postdoctoral Fellow. His research interests are focused on the self-organization of nanoarchitectures and chiral mesoporous nanostructures.

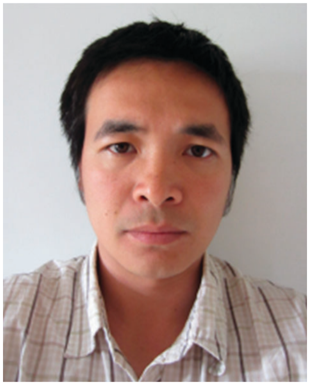

Cao-Thang Dinh

Cao-Thang Dinh is currently a PhD student in the Department of Chemical Engineering at Laval University, supervised by Prof. Trong-On Do. He received his BSc at Hanoi University of Mining and Geology in 2004. He worked at Institute of Chemistry, Vietnamese Academy of Science and Technology from 2005 to 2008. Cao-Thang's current research focuses on the synthesis of multi-functional photocatalysts for the production of solar fuels from water and carbon dioxide.

---

[a] *Department of Chemistry, University of British Columbia, British Columbia, V6T 1Z1, Canada. E-mail: ntdinhc@chem.ubc.ca*

[b] *Department of Chemical Engineering, Laval University, Quebec, G1V 0A6, Canada. E-mail: trong-on.do@gch.ulaval.ca*

diffusion is a powerful way to improve the catalytic activity.[3] There is a general consensus that the active sites of a catalyst can arise from assembly-engineered surfaces and junction-induced interfaces, while the enhancement of reactant diffusion can be established by porous networks. Elegant examples of these materials include periodic composite (*e.g.*, Au–Fe_2O_3) superlattices from particle co-assemblies,[7] Au-tipped CdSe rods prepared by photoreduction,[8] and porous bilayered CeO_2–Pt–SiO_2 nanostructures from particle monolayer assemblies.[9] The particle colloids can organize into nanoarchitectures that may provide collective properties from interparticle arrangements.[10] One of the elegant techniques reported by the Do group shows the organization of SiO_2 spheres coated with uniform titanate nanodisks (TNDs) to produce photonic Au–TiO_2 hollow nanospheres.[11] Further research along these lines focuses on replicating the particles with mesoporous silica templates to construct porous oxide nanostructures.[12]

The global pollution and energy crisis that originated from the overuse of fossil fuels is a grand challenge facing humanity today. Finding renewable fuels based on widely available energy sources to keep up with the energy demand growth while ensuring the increasing standard of living is the most difficult task in the 21st century.[13,14] The utilization of semiconductor-based nanomaterials in the field of photocatalysis has become one of the hottest research topics, as it facilitates the direct conversion of solar energy, the largest renewable energy source, into chemical energy.[5,15,16] This solar energy technology marks a crucial milestone in paving the way for future improvement in producing clean energy alternatives. The solar-to-chemical energy conversion process is also called "artificial photosynthesis", which involves photo-induced water splitting to form hydrogen and oxygen and the light-driven reduction of carbon dioxide to fuels, replicating natural photosynthesis.[17,18] A key determinant of energy storage in the artificial photosynthesis is the efficiency and cost of the man-made photocatalysts.

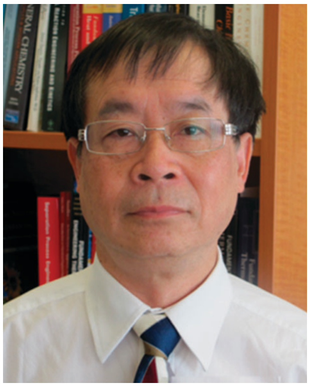

Trong-On Do

Trong-On Do is a full professor in the Department of Chemical Engineering at Laval University, Canada. He received his MSc in 1986 and PhD in 1989 at University of P. and M. Curie (Paris 6, France). After a period at Brunel University (UK) and the French Catalysis Institute (France), he moved to Laval University in 1990. He then spent two years, 1997–1999, as the STA fellow in Japan at Tokyo University before rejoining Laval University as a professor associated with the NSERC Industrial chair. He has published over 120 papers and review articles in refereed journals and holds 5 international patents. He is the recipient of the 2014 Canadian Catalysis Lectureship Award (CCLA).

Generally, a single semiconductor (*e.g.*, TiO_2) exhibits charge photogeneration much faster than charge separation. This behavior leads to rapid electron–hole recombination, giving a poor photocatalytic efficiency.[14] Learning from nature, materials scientists have developed new heterojunctions by using coupling/assembly techniques to produce integrated catalysts that mimic the electron transfer Z-scheme mechanism of ideal plant photosynthesis.[19,20] Synergistic interactions can occur in the integrated catalysts, enabling the creation of solar energy harvesting structures with long charge lifetimes, thus giving exceptional reaction performance. It is accepted that the photocatalytic efficiency may still be low in cases where the semiconductors lack suitable active sites, even if the semiconductor performs carrier separation efficiently. Proper metal-based co-catalysts that act as active sites are commonly integrated into heterostructures to facilitate surface reactions.[21] In this Feature Article, we summarize the recent research efforts of our work and those of other groups, who show the tailoring of the assembly, interfaces, and porosity of nanostructures for the design of integrated catalysts (Fig. 1). An overview of the significant progress in achieving the superior catalytic performance of heterojunctions through synergistic interactions is followed by discussions of efficient solar energy conversion.

Nanoarchitecture assemblies

The oriented assembly of primary particles into three-dimensional (3-D), hierarchical nanostructures offers access to new materials with unique properties.[9] Multi-step templated procedures are commonly applied in fabricating these structures. One notable example was reported by Wang *et al.*,[22] on a two-step procedure for constructing microstructures by first preparing the nanoparticles (Ag, Ag_2S, Ag_2Se) followed by assembling them into microspheres in a microemulsion. Alternatively, one-pot oriented assembly is highly desirable for creating these structures from the particles.[4] The nanoarchitectures are variants of the assembled particles, with the distinction that their pores can be engineered into organized networks.

The surfactant-assisted route has emerged as a versatile tool in controlling the synthesis of uniform particles.[1] The Do group has investigated the use of different methods in surfactant-assisted synthesis to prepare shaped particles that are the units for nanoarchitecture assembly. For example, Dinh *et al.*[23] have exploited uniform, ultrathin TNDs $\sim$22 nm in diameter and $\sim$0.75 nm in thickness prepared by the solvolysis of $Ti(OBu)_4$ in benzyl alcohol–oleylamine–benzyl ether. This is the first preparation of TNDs as elementary units for building nanoarchitectures with plentiful potential uses (presented below). Evidently, the authors observed that TNDs can assemble in ethanol into periodically stacked lamellar structures with a spacing between the disks of $\sim$2.2 nm (Fig. 2a). TNDs were yielded from the growth of TiO_6 octahedral building units generated from the reaction between titanium butoxide (TB) and benzyl alcohol (BA) with the assistance of oleylamine (OM) capping agents in balancing the negative charge of the TNDs. The stacked lamellar

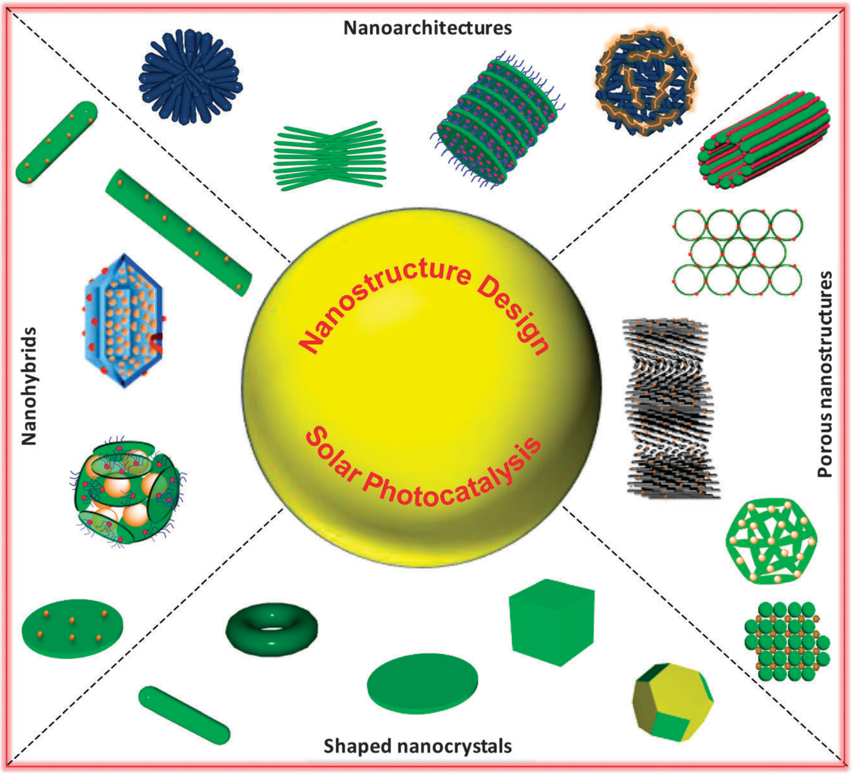

Fig. 1 Tailoring the hierarchical configurations of diverse inorganic nanostructures for the design of integrated catalysts.

organization of the TNDs under the assembly conditions was thought to result from its one-dimensional, ultrathin nanostructure.[23] Another report shows control over the slow aggregation of $LaCO_3OH$ clusters, prepared by the slow thermolysis of La(oleate)$_3$ in water–toluene, into doughnut-shaped mesostructures (Fig. 2b).[24] Stable La(oleate)$_3$ complexes were slowly decomposed in the

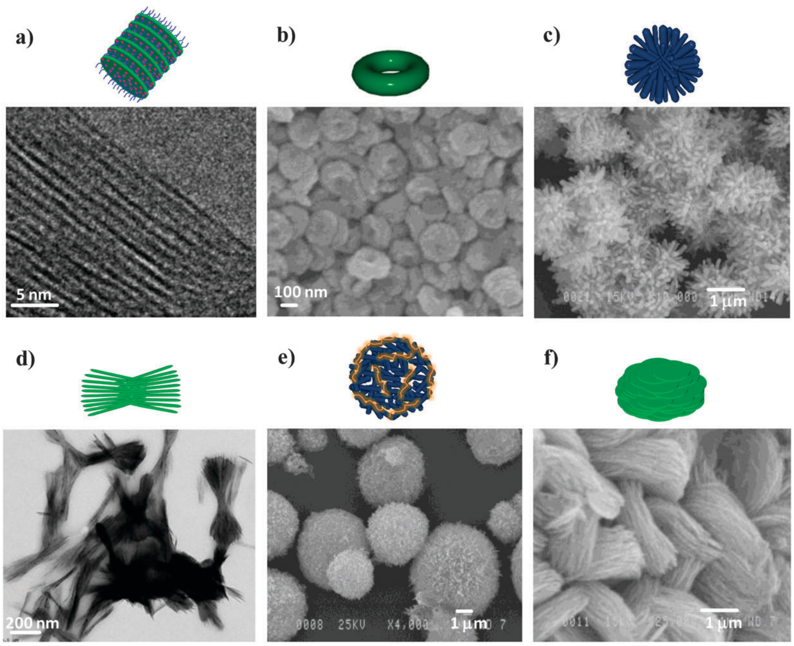

Fig. 2 (a) TND lamellar structures.[23] (b) $LaCO_3OH$ cluster doughnuts.[24] (c) Er_2O_3 rod microflowers.[25] (d) Straw sheaf-shaped Er_2O_3 nanowires.[25] (e) $MnWO_4$ rod microspheres.[26] (f) $MnWO_4$ sheet microspheres.[26] Adapted from ref. 23–26 with permission from Wiley-VCH Verlag GmbH & Co, the American Chemical Society, and the Royal Society of Chemistry.

two-phase water–toluene system containing OM capping agents to generate $LaCO_3OH$ nanoclusters. These OM-capped, colloidal, tiny particles are active building units that self-organize into mesoporous nanoarchitectures with annular shapes to minimize the interface energy. The $LaCO_3OH$ nanocrystals underwent a metathesis upon calcination to transform into porous La_2O_3 doughnuts. These nanodoughnuts resemble $Ce_{1-x}Zr_xO_2$ nanocages prepared by hydrolyzing $ZrOCl_2$ in CeO_2 spheres/glycol.[27] Conversely, the hydrothermal treatment of $Er(NO_3)_3$ in a dodecanoic acid–ethanol–water polar solution facilitated the evolution of Er_2O_3 clusters.[25] Upon controlling the cluster growth using relatively short alkyl capping agents, Er_2O_3 nanoarchitectures with tunable intriguing morphologies were obtained from the fast aggregation of the primary nanowires (Fig. 2c and d), which look similar to those of $LnVO_4$ architectures.[28]

There is considerable current interest in materials that can control the interactions between particles and biomolecules, such as amino acids, peptides and DNA, to assemble them into architectures.[29] Inspired by our previous work on amino acids, these biomolecules are suitable surfactants to organize the oxide particles into nanoarchitectures (Fig. 2e and f).[26] The hydrothermal treatment of a Mn^{2+}–WO_4^{2-}–aminohexanoic acid (AHA)–water mixture enabled $MnWO_4$ nanorods to be obtained with uniform shapes on significant scales. Once AHA molecules are adsorbed on the particles, the stabilized $MnWO_4$ rods become dispersible in water. Free amine and carboxylic acid groups in the capping and residual AHA ligands are available in the reaction solution, thus they can coordinate together to form polypeptides through hydrogen bonds. The discrete nanorods can thereby be cross-linked by hydrogen bonds to assemble into $MnWO_4$ dendrimer-shaped microspheres. Glycine, the simplest amino acid, was also used as a surfactant by Ding *et al.*[30] to prepare TiO_2 hollow structures. Advances in the production of DNA allow its supramolecular bundles to be used as hierarchical platforms to assemble the particles.[31]

Long-range periodic nanostructures

The uniform particles behave like colloids, in that they assemble with long-range order into a periodic structure. Structural coloration arises from 3-D, hierarchical structures as a result of Bragg diffraction of light in a photonic material.[32] Another theme for advancing this property is the coupling of the photonic structure with specific additives to produce new materials with amplified optical properties.[33] There are therefore efforts being made in the development of new synthetic methods to yield these functional materials, which have promise in a variety of areas such as photocatalysis, photovoltaics, and sensors.[32]

The original concept of using an external magnetic field to guide the arrangement of magnetic particles into a photonic nanostructure was pioneered by Yin *et al.*[34] This robust procedure is composed of the preparation of polyacrylate-stabilized Fe_3O_4 clusters followed by the self-organization of these units into periodic nanocluster arrays upon applying the external magnetic field. The magnetic attractive force brings the magnetic particles into ordered linear chains aligned with an external magnetic direction, which results from a balance of the magnetic force and interparticle repulsive force. The iridescent colors of these arrays are observed when the periodicity of the magnetic arrays closely matches the wavelength of the incident light and can appear across the entire visible spectrum under the influence of the external magnetic fields. The authors demonstrated these periodic nanoarrays as responsive photonic materials capable of being transferred into polymer hosts for the design of electronic papers, photonic patterns, and switchable color display sensors.[35,36]

Coupling plasmonic metals with photonic semiconductor crystals is an interesting strategy for constructing efficient photocatalysts.[33] Photonic structures exhibit the slow photon effect by prohibiting the propagation of light with extremely low group velocities in the material. When the slow photon wavelength overlaps with the light absorbed by the incorporated plasmonic metal particles, enhanced light absorption can be obtained. Thus far, metal–semiconductor photonic hybrids, which are primarily based on ordered macrostructures (or inverse opal), have substantially lower surface areas than either their nanoparticles or mesoporous counterparts, preventing them from being efficient photocatalysts. Recently, the Do group designed photonic Au–TiO_2 nanostructures that are constructed from a long-range ordered assembly of thin-shell Au–TiO_2 hollow nanospheres (denoted as Au–TiO_2-3DHNSs) that exhibit iridescent colors (Fig. 3).[11] These materials show not only high surface area, but also photonic behavior originating from the periodic macroscopic voids of the thin-shell hollow nanospheres. This architecture produces multiple light scattering and slow photon effects to enhance the surface plasmon resonance of Au particles, thus giving visible light-responsive Au–TiO_2-3DHNSs. As a result, these new structures exhibit several-fold higher photocatalytic activity compared to Au–TiO_2 nanopowders, as illustrated by the example of the visible light-driven photodecomposition of isopropanol into CO_2.

The incorporation of quantum dots (QDs) into photonic crystals affords attractive semiconducting photonic materials useful for optoelectronic technology.[38] QDs-loaded photonic crystals can be commonly fabricated by repeatedly infiltrating QDs into inverse opals.[38] This procedure involves time-consuming steps and uses expensive templates. Chiral nematic cellulose nanocrystals (CNCs) with structural colors can be used as alternative liquid-crystalline (LC) templates to reinforce photonic porous nanomaterials. This primary concept was recently reported by Nguyen *et al.*[37] through a one-step co-assembly of water-dispersible polyacrylic acid (PAA)–mercaptopropionic acid (MPA)-stabilized CdS QDs with $Si(OCH_3)_4$ and CNC aqueous dispersion to generate chiral nematic CdS–SiO_2–CNC composites. The subsequent removal of the CNC template by controlled calcination of the composites generated free-standing luminescent, iridescent chiral mesoporous CdS–SiO_2 films (Fig. 4). The semiconducting properties of the photonic films remained intact as they underwent luminescence quenching by trinitrotoluene vapor. These films, which can be prepared using renewable CNCs, may potentially be used as hosts, by embedding

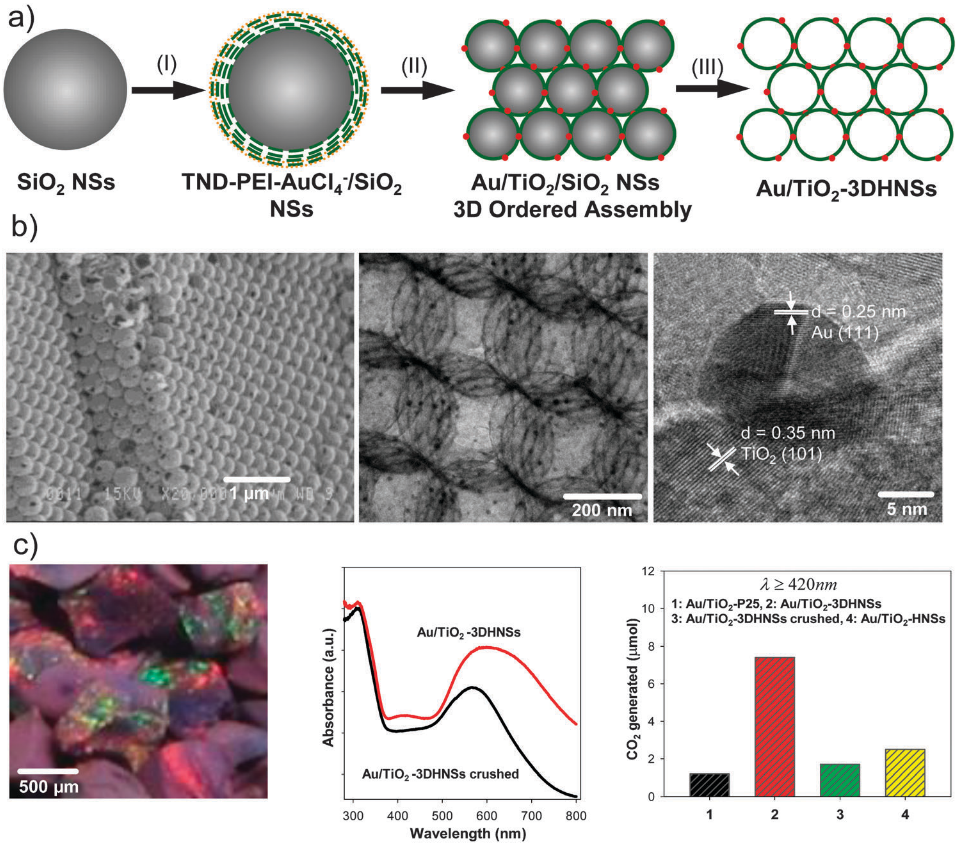

Fig. 3 (a) Synthetic procedure for the design of Au–TiO$_2$-3DHNSs. (b, from left to right) SEM, TEM and HRTEM of the Au–TiO$_2$-3DHNSs. (c, from left to right) Photograph, UV-vis spectrum and visible light isopropanol photodecomposition of Au–TiO$_2$-3DHNSs in comparison with Au–TiO$_2$ of different structures.[11] Adapted from ref. 11 with permission from Wiley-VCH Verlag GmbH & Co.

TiO$_2$ particles within their pores, to produce CdS-contacted TiO$_2$ structures amenable to photocatalysis. There was a previous attempt to incorporate hydrophobic CdSe–ZnS QDs into a cellulose triacetate matrix, but the resulting composites showed neither photonic chirality nor porosity.[39] Techniques using other biopolymers, such as lipids and peptides, as soft templates have been implemented to make TiO$_2$,[40] Co$_3$O$_4$ and ZnO[41] hierarchical replicas.

Particle coupling-induced interfaces

Interparticle interfaces in a nanostructure have favorable effects on the catalytic performance.[2] It is desirable to introduce the interfaces into nanostructures by applying the appropriate combination of constituents. Busbee *et al.*[42] was early to propose the surface growth of HAuCl$_4$ on Au spherical seeds to evolve nanorods. Later, modified surface selective growth routes, such as photoreduction, cation exchange, and surface modification, were studied extensively by different groups and in our recent research for the design of the nanohybrids.

UV light-induced growth was first reported by Pacholski *et al.*[43] for the synthesis of Ag–ZnO nanorods. The authors proposed that electrons generated on semiconductor surfaces under UV excitation can reduce Ag$^+$ in the ZnO particle dispersion into deposited Ag clusters. The successful invention of this method of photodeposition without the aid of organic molecular bridges is the great breakthrough that could be extended to other semiconductor-based composites. Later, Mokari *et al.*[8] selectively photodeposited Au clusters at the tips of CdSe rods. Recently, the Do group presented the photoreductive synthesis of metal–semiconductor nanomaterials. Evidently, the UV irradiation of an ethanol–toluene dispersion of oleic acid (OA)-capped TiO$_2$ nanorods and AgNO$_3$ was carried out to obtain Ag–TiO$_2$ hybrids (Fig. 5a) that show enhanced photodegradation of methylene blue.[44] This photodeposition was used by Lu *et al.*[45] to synthesize Ag–TiO$_2$ nanorods for the design of photovoltaic devices. This route presents the feasibility of precise control over the population of the uniform metal clusters on the individual TiO$_2$ particles.

The ion-exchange process was recently used by the Do group for the selective substitution of cations ligated on the particles with target ligands in aqueous solution, for the controlled deposition of the clusters on TNDs (Fig. 5b and c).[23,46,49] The authors performed the cation exchange of oleylamine-capped TNDs with tetraethylammonium (TEA) ligands in water. The water-dispersible TEA-stabilized TNDs obtained can be solely used as ideal islands for constructing nanohybrids in water. Cluster (metal, metal sulfide)-exchanged TND heterostructures can be obtained by the partial replacement of TEA molecules on

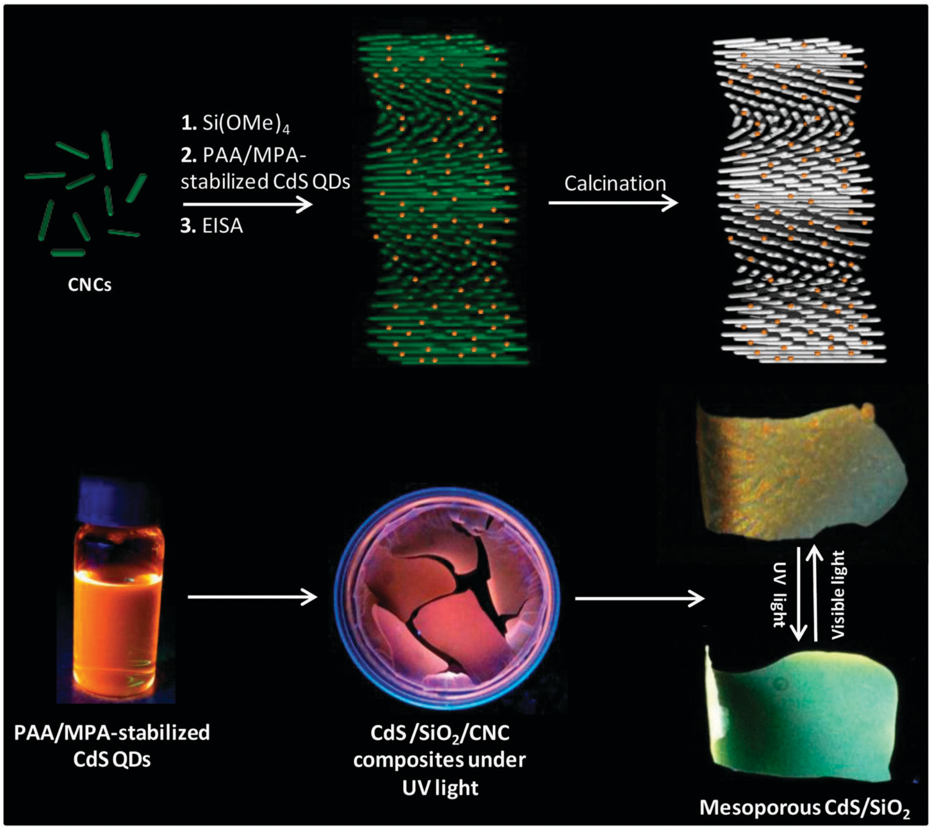

Fig. 4 Co-assembly of CdS QDs with Si(OCH$_3$)$_4$ and cellulose LCs to produce chiral mesoporous CdS–SiO$_2$ films. The films were photographed under visible light and UV light.[37] Adapted from ref. 37 with permission from Wiley-VCH Verlag GmbH & Co.

TNDs by metal cations. The metal cations were strongly attached to the TND's surfaces through electrostatic interactions and then grew to 2–4 nm deposited metal clusters without any aggregation. The water-dispersible TND-based nanohybrids with a synergistic configuration show enhanced photodegradation of methylene blue. The cation exchange was also applied by Luo *et al.*[50] to selectively deposit CdSe on polystyrene-templated TiO$_2$ opals for H$_2$ generation.

The organic molecule linkers can function as bridges to assist the coupling of discrete particles into nanocomposites. Bao *et al.*[51] used cysteine to modify Fe$_3$O$_4$ particle surfaces and then decorated them with Au particles through its amine groups. The Do group showed that aminohexanoic acid and hexamethylenediamine were bifunctional linkers for the design of water-dispersible nanohybrids (Fig. 5d–f).[47,48] Once these linkers were stabilized on the particle surfaces, the carboxylic acid and amine groups not only provided growth sites for particle deposition but also inhibited any agglomeration. The selective deposition was performed by attaching metal ions to the functional groups of amino acid or diamine molecules stabilized on the nanoparticles and subsequently reducing them to metallic clusters using a reducing agent. This route was used with different nanocomposites such as Au–MnWO$_4$ rods, Au–CoWO$_4$ octahedra, Ag–La$_2$(MoO$_4$)$_3$ sheets, Ag–TiO$_2$ belts, and Cu–CeO$_2$ cubes. The synergistic interactions in the CeO$_2$ nanocubes coupled with 2.9–10.0 wt% Cu clusters resulted in a CO oxidation activity substantially higher than that of bare CeO$_2$ nanocubes.[48]

Engineering porosity into nanostructures

Opening pores within the nanostructures can amplify the access of the reactants to the surface reactions, in principle, improving the catalytic performance.[3] There are several ways to engineer the porosity: one can reconstruct nanohybrid colloids to open pores, and the former can be porous nanocomposites obtained from casting. Notably, porous non-siliceous nanomaterials can be prepared by either assembling the discrete particles into an organized porous system or infiltrating a porous hard template with a precursor followed by calcination and template removal.[12] Another route involves assembling the polymeric template with a precursor in the process to prepare porous nanostructures.[12]

The assembled organization was proposed by Shevchenko *et al.*[7] to produce composite superlattices from particle colloids by ordering the interparticle interfaces. Yamada *et al.*[9] modified this protocol to design bilayered catalysts with enhanced interfaces by sequentially assembling Pt and CeO$_2$ nanocube monolayers on the substrates. The Do group extended this theme to construct mesoporous metal–oxide nanostructures. For example,

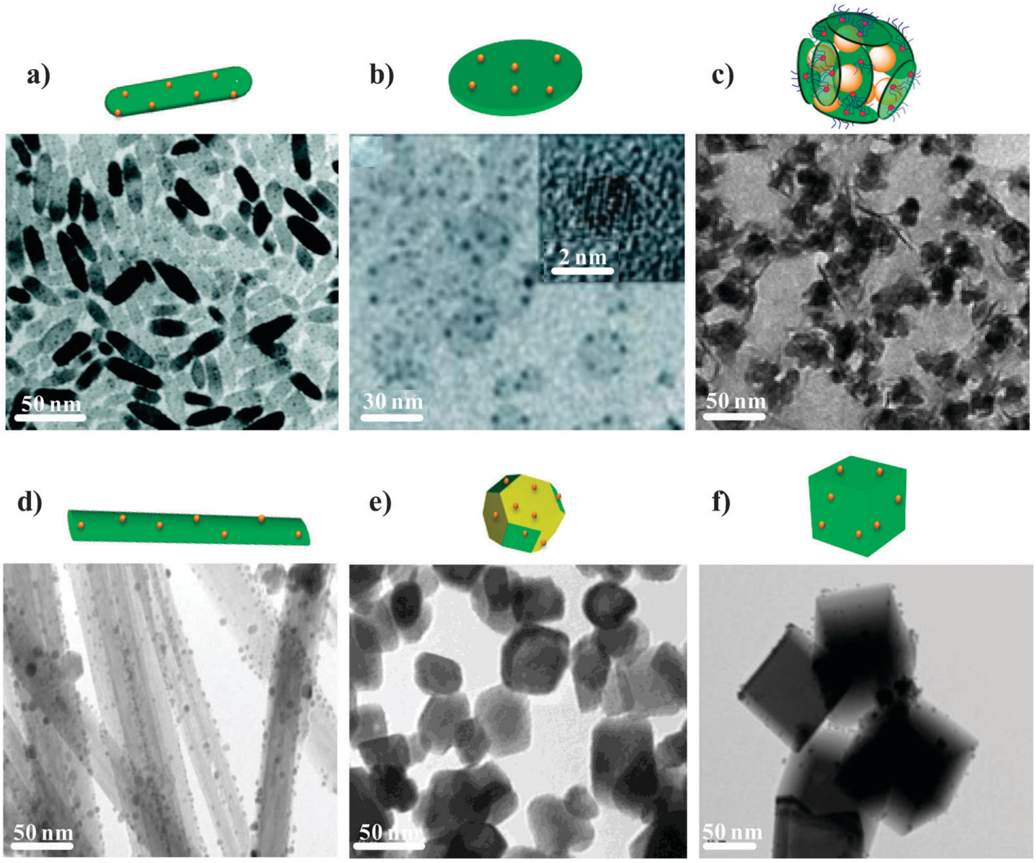

Fig. 5 (a) Ag–TiO_2 nanorods prepared using photoreduction.[44] (b) Ag–TND composites prepared using cation exchange.[23] (c) Ni–TND–CdS composites prepared using sequential cation exchange and photoreduction.[46] Ag–TiO_2 belts (d), Au–$CoWO_4$ octahedra (e), Cu–CeO_2 cubes (f) all prepared using amino acid- or diamine-surface modification.[47,48] Adapted from ref. 23, 44 and 46–48 with permission from the American Chemical Society, Wiley-VCH Verlag GmbH & Co, the Royal Society of Chemistry, the American Chemical Society, and Elsevier.

the co-assembly of OA-capped metal (Au, Cu) with OA-capped oxide (TiO_2, ZrO_2) particles was accomplished to make metal–oxide nanocomposites.[52] The removal of the stabilized capping agents from the composites by calcination generated mesoporous structures connected between the metal and oxide nanoarrays and ensured the retention of the sizes of the pristine particles. These porous nanocomposites show enhanced CO catalytic activity compared to the individual components, probably due to the porosity and the presence of metal–oxide interfaces in the material.

Once again, Dinh *et al.*[23] used the TEA-exchanged TNDs as brick units to construct mesoporous supports. The TEA-stabilized TNDs were sequentially exchanged with metal cations (*e.g.*, Ag^+, Cu^{2+} and Ni^{2+}) to form precipitates of metal cluster-exchanged TND nanohybrids in water. In basic media, the cluster-deposited TND colloids can organize into mesoporous hybrids with large voids, formed due to good connectivity between the edges of the nanodisks. The engineering of porous materials with surface areas of 250–320 $m^2\ g^{-1}$ and pore sizes of 4.9–9.3 nm with TNDs can be achieved depending on the sizes of the TNDs employed in the preparation.

Hard templating techniques are proven to be successful for preparing porous oxide nanostructures. These porous nanomaterials can be obtained by repeatedly infiltrating mesoporous silica with a metal salt precursor followed by calcination and template removal. The apparent obstacle of this impregnation method is the time-consuming procedure. Yen *et al.*[53,54] recently developed a one-step hard templating route to produce mesoporous nanocomposites (Fig. 6). The procedure involves refluxing a hexane mixture containing binary metal nitrates and mesoporous silica, to melt the metal salts in hexane and cause infiltration of the porous silica in one step. Mesoporous mixed oxide nanostructures can be obtained by calcining the metal ion–silica composites followed by etching the silica away. This convenient pathway was applied to truly replicate the high-surface-area mesoporous oxide nanoarrays of different composites, including $NiFe_2O_4$, $CuFe_2O_4$, Cu–CeO_2, and Cu–NiO. With the combination of their mesoporosity and multiple components, the mesoporous 30 wt% Cu–CeO_2 nanostructures showed complete CO oxidation at ~40 °C.[54]

Integrated photocatalysts for solar energy conversion

Semiconductor-based nanocatalysts have the potential for use in solar energy conversion, which offers a way to alleviate

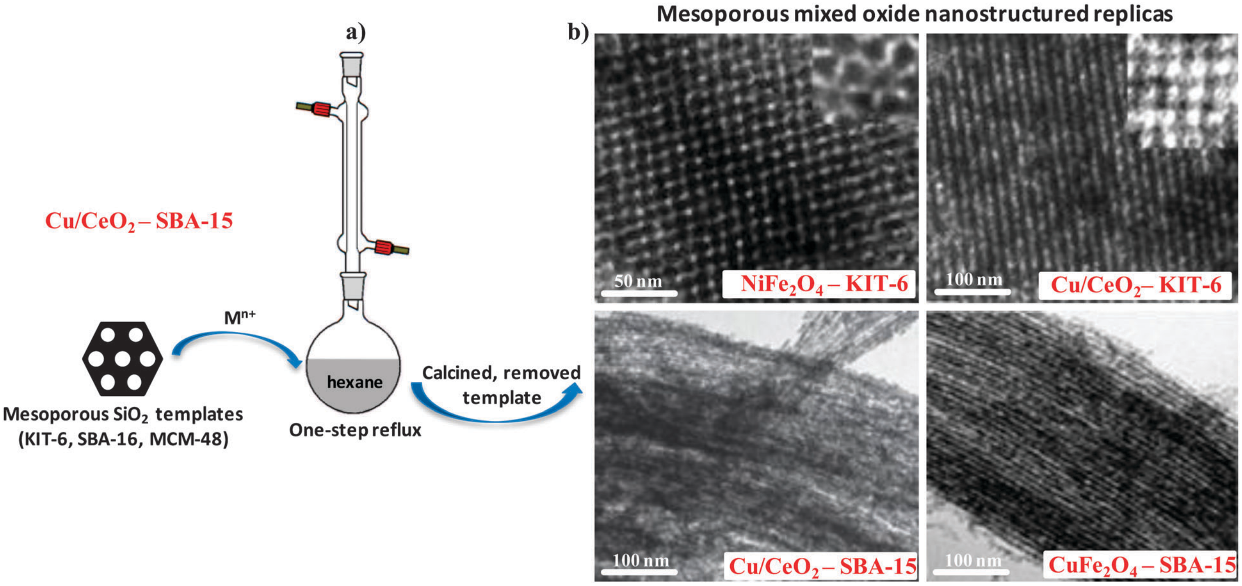

Fig. 6 One-step replication of mesoporous mixed oxide nanostructures with silica hard templates.[53] Adapted from ref. 53 with permission from the Royal Society of Chemistry.

emerging energy and environmental issues. The most significant achievement of this alternative technology is engineering semiconductors with narrow bandgap energy and interfacial contacts that are pivotal in producing integrated photocatalysts with enhanced power-conversion efficiency. The carbon-free production of H_2 through solar water splitting is widely recognized as the most green and economic method to produce valuable fuels. CO_2 photoreduction may not only alleviate the problem of CO_2 emissions but also convert CO_2 and sunlight into energy, in principle. Despite being simple reactions, these solar energy conversions are slow multi-electron processes that need to be catalyzed. The original concept and reaction mechanism of using TiO_2 for photo-induced water splitting and CO_2 reduction were easily demonstrated in the 1970s.[55,56] Considering the electronic states and high-density atomic arrangements at the nanocrystal surfaces, the photocatalytic activity of TiO_2 nanostructures is primarily determined by high-energy surfaces.[57] Studies on the shape-dependence of photocatalytic activity over TiO_2 nanocrystals revealed that exposed, chemically active {001} facets have much greater reactivity than lower energy facets.[58,59] Photocatalytic H_2-production activity was greatly improved by doping nitrogen into exposed {001}-faceted TiO_2 nanosheets.[60] Yu *et al.*[61] demonstrated that engineering the co-exposure of the {101} and {001} facets with an optimal ratio of 45 : 55 in anatase TiO_2 nanocrystals with a surface heterojunction affords active photocatalysts that show a great enhancement in the selective reduction of CO_2 into CH_4. These interesting findings have already shown TiO_2 materials to be industrially important semiconductors and are a major creative breakthrough for extending solar energy conversion abilities to other semiconductors.[62]

The development of solar fuels requires using natural sunlight, however, the pure TiO_2 materials exhibit low adsorption ($\leq 5\%$) in the solar spectrum, thus giving a poor energy conversion efficiency. In terms of geometry-dependent catalytic properties, seeking out affordable approaches to producing integrated catalysts with engineered nanostructures is a key goal for tackling this obstacle. In nature, plants can perform sunlight-to-chemical energy conversion directly under ambient conditions using what is known as a "Z-scheme", driven by the absorption of two photons on two different reaction centers.[14] Materials scientists are trying to design heterojunction semiconductors for efficient energy production that exhibit an electron transfer mechanism similar to that between the components in ideal plant photosynthesis. The heterojunctions can function as integrated photocatalysts with exceptional optoelectronic properties: sunlight harvesting, prolongated electron–hole separation, and the shuttling of photoexcited electrons on co-catalysts.[14,20] The artificial mechanism was clearly reported by Tada *et al.*[63] for a CdS–Au–TiO_2 Z-scheme system that contains a vectorial electron-transfer path and consequently superior H_2 evolution.

The stability of the composite materials, product selectivity, co-catalysis, and relationship between the structural geometric features and bandgap energy are worth considering for the design of solar nanostructured catalysts. There is a growing demand for new paradigms to prepare coupled semiconductors with long-lived electron–hole separation and a slow charge recombination rate to advance toward more efficient solar energy conversion. Amirav *et al.*[64] proposed the enhancement of H_2 generation by introducing interfaces into Pt-tipped CdS–CdSe nanorods. Coupling narrow-bandgap semiconductors with Pt particles built bridges of interfacial contacts that transfer charges across junctions, resulting in the harvesting of visible light and enhancing H_2 evolution. Silicon (Si) nanowires junctioned with additives are an attractive materials choice for constructing artificial leaves for future photosynthesis.[6] Yang *et al.*[65] performed the coupling of Si nanowires with

TiO_2 nanobranches to produce a dual light-absorber system that can be imagined as artificial forest trees capable of releasing H_2 on a visible light-responsive Si photocathode and O_2 on a UV-responsive TiO_2 photoanode. Xiang *et al.*[66] proposed positive synergetic effects between MoS_2 and graphene in TiO_2 nanoparticle-decorated supports, which give access to high-performance integrated photocatalysts for highly efficient H_2 evolution. Recent attempts in achieving visible light-driven CO_2 photoreduction show that enhanced activity and selectivity can be obtained by introducing the interfaces into heterojunction catalysts. Ola *et al.*[67] found compounds of H_2, CH_3OH, CH_3CHO and C_2H_5OH derived from CO_2 photoreduction over Cu–TiO_2 heterojunctions threaded with optical fibres. Wang *et al.*[68] proposed active Pt–TiO_2 nanohybrid films for high CO_2 photoreduction efficiency with the selective formation of CH_4. These reports reveal that the presence of the interfaces in the integrated nanocatalysts leads to enhanced photocatalytic performance.

The introduction of metal-based species as reductive and oxidative co-catalysts into semiconductors results in the enhancement of photoactivity and selectivity.[69] Cocatalysts, such as metal clusters and metal–organic complexes, integrated into photocatalysts provide electron traps to shuttle photoexcited electrons to reagents to perform reaction processes.[21] Han *et al.*[70] proposed the role of Ni^{2+}–dihydrolipoic acid co-catalysts as solar light absorbers adsorbed on CdSe particles for proton reduction with ascorbic acid to produce H_2. Ong *et al.*[71] reported the decoration of Ni co-catalysts and TiO_2 semiconductors on carbon nanotubes to obtain visible light-responsive active photocatalysts for the photoreaction of CO_2 to CH_4. The Do group proposed a new type of hollow PtO_x–TiO_2 hybrid nanostructure with a thin wall (∼15–30 nm) templated by metal organic frameworks (MOFs) (Fig. 7).[72] The subsequent deposition of the PtO_x co-catalysts was performed on two opposing sides of the calcined hollow structures to produce hollow nanohybrids. These novel materials showed high visible light-driven H_2 evolution, which could result from improved charge separation, likely due to its thin wall, porosity, and the isolated location of the two different co-catalysts on the hollow frameworks. Zhou *et al.*[73] performed the replication of 3-D hierarchical porous perovskite titanate $ATiO_3$ (A = Sr, Ca, Pb) architectures with natural leaves as the hard template. Upon the removal of the template in the composites by calcination, the authors obtained biomimetic materials in the form of artificial leaves that work efficiently as full-sunlight-driven photocatalysts with highly hierarchical porous structures for the photoreduction of CO_2 to CO and CH_4 with an enhanced power-conversion efficiency.

The visible light photoreduction of CO_2 performed over three-component CdSe/Pt/TiO_2 photocatalysts was reported by Wang *et al.*[74] The roles of the interfaces and Pt co-catalysts in the heterojunctions determined the reaction yields of the gas-phase products, with CH_4 as the primary product. Recently, the Do group[46,49] reported a water-dispersible noble-metal free photocatalytic system, metal sulfide–TND–Ni, that shows superior reactivity originating from the introduction of the interfaces and co-catalysts into a three-component heterojunction. This unprecedented junction gave access to active photocatalysts for sunlight-driven H_2 evolution with exceptional longevity, maintaining high activity with no decrease after five recycling experiments (Fig. 8). Under visible light illumination,

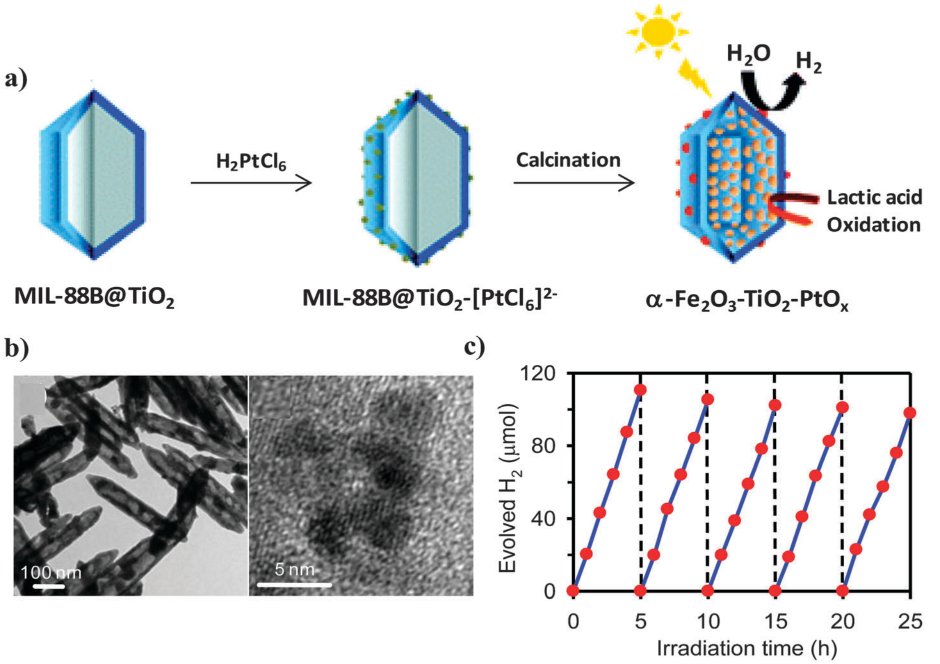

Fig. 7 (a) Formation of Fe_2O_3–TiO_2–PtO_x hollow nanostructures using MOF hard templates. (b) Different-magnification TEM images of the Fe_2O_3–TiO_2–PtO_x hollow structures. (c) Visible light-driven H_2 evolution of the Fe_2O_3–TiO_2–PtO_x photocatalysts.[72] Adapted from ref. 72 with permission from the Royal Society of Chemistry.

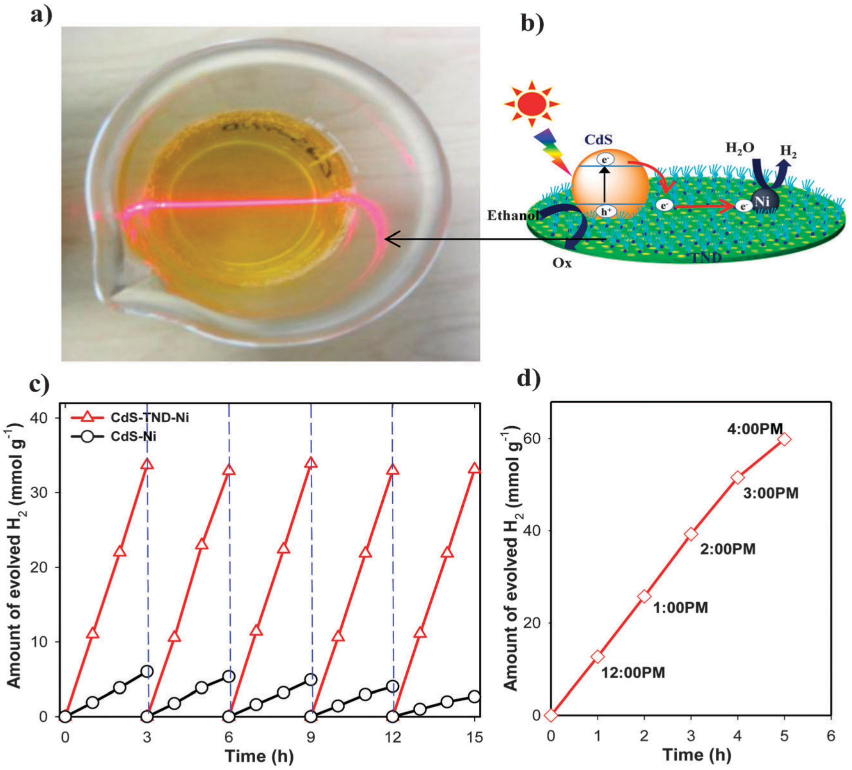

Fig. 8 (a) CdS–TND–Ni heterojunction aqueous dispersion. (b) Transfer mechanism of charge carriers in CdS–TND–Ni for solar H_2 evolution. (c) Comparative H_2 evolution from CdS–TND–Ni and CdS–Ni catalysts under visible light. (d) Solar energy-driven H_2 production from CdS–TND–Ni.[46] Adapted from ref. 46 with permission from the Royal Society of Chemistry.

the CdS–TND–Ni nanocatalysts generated H_2 at an average rate of 11.038 mmol g^{-1} h^{-1} from ethanol–water,[46] which makes them some of the most highly active metal sulfide photocatalysts in the absence of noble metal co-catalysts.[75] In the CdS–TiO_2–Ni system, Ni clusters and CdS particles are localized at the interlayers between TiO_2 disks, which leads to the electrons photogenerated from the CB of CdS being injected into the CB of the TNDs, and then to the capping Ni co-catalysts for H_2 evolution. The authors speculated that the outstanding features of large-contact-area interfaces, good dispersion of deposited Ni clusters, and water dispersion are the important factors of these heterojunctions for contributing to superior H_2 evolution. It is conceptually new to begin with uniform TNDs in making new nanomaterials, as our works have demonstrated.[23,46,49] The one-dimensional TiO_2 nanodisks are being studied extensively for the development of solar photoelectrochemical hybrid cell films as efficient photoanode electrodes *via* multilayered assembly on functionalized substrates. In this context, combined with their earth-abundance, photostability, and synthetic feasibility, these materials have a great chance of being applied in the photocatalytic production of solar fuels.

Conclusions and outlook

In this Feature Article, we summarized the recent progress reported in our research and that of other research groups in tailoring the assembly, interfaces, and porosity of well-defined inorganic nanostructures and demonstrated the synergistic effects of integrated catalysts on the reaction performance. The main criterion in dealing with desirable surfactant-assisted routes is to produce well-defined nanostructures with precise control over the surface properties. The controlled growth of surface-functionalized nanoclusters is important for speculating the construction of the hierarchically organized nanostructures. Interparticle interfaces induced by the clever coupling of constituents can donate surface sites in heterojunction nanostructures to enhance catalytic activity. We aim to present selective growth concepts to bring single particles into heterojunctions, such as Ag-photodeposited TiO_2 nanorods, metal sulfide-exchanged TiO_2 nanodisks, and metal (Ag,Au)–amino acid, diamine functionalized oxide (CeO_2, $MnWO_4$, $La_2(MoO_4)_3$) nanohybrids. Engineering porosity into the nanostructures has been performed by templating, and is capable of amplifying reactant diffusion to enhance reaction performance. We presented significant attempts to exploit the self-construction of the particles into mesoporous nanostructures such as metal (Ag,Au)–oxide (CeO_2, ZrO_2, TiO_2) nanocomposites, chiral CdS-encapsulated SiO_2 thin films, and silica-templated mixed oxide (*e.g.*, Cu–CeO_2) nanosized replicas.

The conversion of energy from photons in sunlight to chemicals is the most promising technology for the production of renewable fuels in the future. The nanostructured features of the engineered nanomaterials were shown, through the development of synergistic interactions, to boost the activity and selectivity in solar energy conversion for solar water splitting, CO_2 photoreduction, and organic photodecomposition. We discussed the synergistic effects of the assembly-induced interfaces and pores involved in the engineered nanostructures on the enhanced reactivity *via* inspiration from artificial photosynthesis. Along with expressive achievements of the integrated catalysts available from the literature, our recent works highlighted the successful development of integrated catalysts, *e.g.*, $CdS–TiO_2–Ni$ disks and $Fe_2O_3–TiO_2–PtO_x$ hollow structures, for superior H_2 evolution and $Au–TiO_2$ hollow nanocrystals for the decomposition of volatile organic compounds (VOCs) under visible light. We demonstrated the layer-by-layer assembly of TiO_2 nanodisks with SiO_2 nanospheres to obtain ordered thin-shell $Au–TiO_2$ hollow nanospheres for the enhanced photodecomposition of VOCs. Tailoring the structural geometry of the photocatalysts decorated with metal-based co-catalysts leads to an enhancement in energy conversion efficiency. Our studies showed that Ni co-catalysts incorporated selectively into the $CdS–TiO_2$ hybrid nanodisks yield water-dispersible heterojunctions that are highly active for natural sunlight-driven water splitting. The integration of PtO_x co-catalysts into $Fe_2O_3–TiO_2$ hollow nanostructures afforded new visible light-driven photocatalysts showing a high H_2 generation rate.

In terms of their attributes of superior catalytic performance and long-term durability, the economical, active photocatalysts open up practical opportunities to develop artificial photosynthesis and other fields, such as the photodegradation of persistent organic pollutants and photovoltaic cells for the generation of electricity. The great evolution of solar fuel technology over 40 years, since the first demonstration of TiO_2 photocatalysts, has been acknowledged. However, water photosplitting still requires further improvement in order to approach the record efficiencies achieved by semiconductor solar fuel devices to compete with fossil fuels. As the conversion efficiency of CO_2 into valuable energy-bearing hydrocarbons is still low, since CO_2 is a highly stable molecule, the component- and structural geometry-dependent photocatalytic properties and the cost of the solar energy-driven photocatalysts have not yet been satisfactorily investigated and many questions remain unanswered. It is therefore necessary to clarify the link between the photocatalytic efficiency and cost-effectiveness of solar junction devices. Continuing research in the development of new nanomaterials will certainly facilitate the tackling of unaddressed challenges and translation of artificial solar fuel generation technology into reality in the upcoming decade. Once the efficient solar energy-driven nanocatalysts are widely available in industrial processing activities, alternative technology will play a role in producing green fuels, reducing CO_2 emissions, serving our needs, and saving the planet.

Conflicts of interest

The authors declare no competing financial interests.

Acknowledgements

We are grateful to the Natural Sciences and Engineering Research Council (NSERC) of Canada for funding. T.D.N and C.T.D thank NSERC for a postdoctoral fellowship and les fonds de recherche du Québec (FQRNT) for an excellence scholarship, respectively.

Notes and references

1 B. L. Cushing, V. L. Kolesnichenko and C. J. O'Connor, *Chem. Rev.*, 2004, **104**, 3893–3946.
2 S. Surnev, A. Fortunelli and F. P. Netzer, *Chem. Rev.*, 2013, **113**, 4314–4372.
3 Q. Zhang, I. Lee, J. B. Joo, F. Zaera and Y. Yin, *Acc. Chem. Res.*, 2013, **46**, 1816–1824.
4 Z. Nie, A. Petukhova and E. Kumacheva, *Nat. Nanotechnol.*, 2010, **5**, 15–25.
5 X. Chen, S. Shen, L. Guo and S. S. Mao, *Chem. Rev.*, 2010, **110**, 6503–6570.
6 C. Liu, N. P. Dasgupta and P. Yang, *Chem. Mater.*, 2014, **26**, 415–422.
7 E. V. Shevchenko, D. V. Talapin, N. A. Kotov, S. O'Brien and C. B. Murray, *Nature*, 2006, **439**, 55–59.
8 T. Mokari, C. G. Sztrum, A. Salant, E. Rabani and U. Banin, *Nat. Mater.*, 2005, **4**, 855–863.
9 Y. Yamada, C. K. Tsung, W. Huang, Z. Huo, S. E. Habas, T. Soejima, C. E. Aliaga, G. A. Somorjai and P. Yang, *Nat. Chem.*, 2011, **3**, 372–376.
10 S. H. Kim, J. M. Lim, S. K. Lee, C. J. Heo and S. M. Yang, *Soft Matter*, 2010, **6**, 1092–1110.
11 C. T. Dinh, H. Yen, F. Kleitz and T. O. Do, *Angew. Chem., Int. Ed.*, 2014, **53**, 6618–6623.
12 D. Gu and F. Schuth, *Chem. Soc. Rev.*, 2014, **43**, 313–344.
13 U. Banin, Y. B. Shahar and K. Vinokurov, *Chem. Mater.*, 2014, **26**, 97–110.
14 Y. Tachibana, L. Vayssieres and J. R. Durrant, *Nat. Photonics*, 2012, **6**, 511–518.
15 W. Tu, Y. Zhou and Z. Zou, *Adv. Mater.*, 2014, **26**, 4607–4626.
16 J. Low, S. Cao, J. Yu and S. Wageh, *Chem. Commun.*, 2014, **50**, 10768–10777.
17 N. S. Lewis and D. G. Nocera, *Proc. Natl. Acad. Sci. U. S. A.*, 2006, **103**, 15729–15735.
18 J. Michl, *Nat. Chem.*, 2011, **3**, 268–269.
19 R. Costi, A. E. Saunders and U. Banin, *Angew. Chem., Int. Ed.*, 2010, **49**, 4878–4897.
20 P. Zhou, J. Yu and M. Jaroniec, *Adv. Mater.*, 2014, **26**, 4920–4935.
21 J. Yang, D. Wang, H. Han and C. Li, *Acc. Chem. Res.*, 2013, **46**, 1900–1909.
22 D. Wang, T. Xie, Q. Peng and Y. Li, *J. Am. Chem. Soc.*, 2008, **130**, 4016–4022.
23 C. T. Dinh, Y. Seo, T. D. Nguyen, F. Kleitz and T. O. Do, *Angew. Chem., Int. Ed.*, 2012, **51**, 6608–6612.
24 T. D. Nguyen, C. T. Dinh and T. O. Do, *Inorg. Chem.*, 2011, **50**, 1309–1320.
25 T. D. Nguyen, C. T. Dinh and T. O. Do, *ACS Nano*, 2010, **4**, 2263–2273.
26 T. D. Nguyen, D. Mrabet, T. T. D. Vu, C. T. Dinh and T. O. Do, *CrystEngComm*, 2011, **13**, 1450–1460.
27 X. Liang, X. Wang, Y. Zhuang, B. Xu, S. Kuang and Y. Li, *J. Am. Chem. Soc.*, 2008, **130**, 2736–2737.
28 H. Deng, C. Liu, S. Yang, S. Xiao, Z. K. Zhou and Q. Q. Wang, *Cryst. Growth Des.*, 2008, **8**, 4432–4439.
29 M. B. Dickerson, K. H. Sandhage and R. R. Naik, *Chem. Rev.*, 2008, **108**, 4935–4978.
30 S. Ding, F. Huang, X. Mou, J. Wu and X. Lu, *J. Mater. Chem.*, 2011, **21**, 4888–4892.
31 R. J. Macfarlane, B. Lee, M. R. Jones, N. Harris, G. C. Schatz and C. A. Mirkin, *Science*, 2011, **334**, 204–208.
32 C. I. Aguirre, E. Reguera and A. Stein, *Adv. Funct. Mater.*, 2010, **20**, 2565–2578.
33 S. Kim, A. N. Mitropoulos, J. D. Spitzberg, H. Tao, D. L. Kaplan and F. G. Omenetto, *Nat. Photonics*, 2012, **6**, 818–823.
34 J. Ge and Y. Yin, *Adv. Mater.*, 2008, **20**, 3485–3491.
35 H. Kim, J. Ge, J. Kim, S. Choi, H. Lee, H. Lee, W. Park, Y. Yin and S. Kwon, *Nat. Photonics*, 2009, **3**, 534–540.

36 M. Wang, L. He, Y. Hu and Y. Yin, *J. Mater. Chem. C*, 2013, **1**, 6151–6156.
37 T. D. Nguyen, W. Y. Hamad and M. J. MacLachlan, *Adv. Funct. Mater.*, 2014, **24**, 777–783.
38 K. Aoki, D. Guimard, M. Nishioka, M. Nomura, S. Iwamoto and Y. Arakawa, *Nat. Photonics*, 2008, **2**, 688–692.
39 T. Abitbol and D. Gray, *Chem. Mater.*, 2007, **19**, 4270–4276.
40 S. Liu, L. Han, Y. Duan, S. Asahina, O. Terasaki, Y. Cao, B. Liu, L. Ma, J. Zhang and S. Che, *Nat. Commun.*, 2012, **3**, 1215.
41 H. Ceylan, C. O. Akgun, T. S. Erkal, I. Donmez, R. Garifullin, A. B. Tekinay, H. Usta, N. Biyikli and O. M. Guler, *Sci. Rep.*, 2013, **3**, 2306.
42 B. D. Busbee, S. O. Obare and C. J. Murphy, *Adv. Mater.*, 2003, **15**, 414–416.
43 C. Pacholski, A. Kornowski and H. Weller, *Angew. Chem., Int. Ed.*, 2004, **116**, 4878–4881.
44 C. T. Dinh, T. D. Nguyen, F. Kleitz and T. O. Do, *ACS Appl. Mater. Interfaces*, 2011, **3**, 2228–2234.
45 Q. Lu, Z. Lu, Y. Lu, L. Lv, Y. Ning, H. Yu, Y. Hou and Y. Yin, *Nano Lett.*, 2013, **13**, 5698–5702.
46 C. T. Dinh, M. H. Pham, F. Kleitz and T. O. Do, *J. Mater. Chem. A*, 2013, **1**, 13308–13313.
47 T. D. Nguyen, C. T. Dinh and T. O. Do, *Nanoscale*, 2011, **3**, 1861–1873.
48 T. D. Nguyen, C. T. Dinh, D. Mrabet, T. M. N. Tran and T. O. Do, *J. Colloid Interface Sci.*, 2013, **394**, 100–107.
49 C. T. Dinh, M. H. Pham, Y. Seo, F. Kleitz and T. O. Do, *Nanoscale*, 2014, **6**, 4819–4829.
50 J. Luo, S. K. Karuturi, L. Liu, L. T. Su, A. L. Y. Tok and H. J. Fan, *Sci. Rep.*, 2012, **2**, 451.
51 J. Bao, W. Chen, T. Liu, Y. Zhu, P. Jin, L. Wang, J. Liu, Y. Wei and Y. Li, *ACS Nano*, 2007, **1**, 293–298.
52 D. Mrabet, M. H. Zahedi-Niaki and T. O. Do, *J. Phys. Chem. C*, 2008, **112**, 7124–7129.
53 H. Yen, Y. Seo, R. G. Nicolas, S. Kaliaguine and F. Kleitz, *Chem. Commun.*, 2011, **47**, 10473–10475.
54 H. Yen, Y. Seo, S. Kaliaguine and F. Kleitz, *Angew. Chem., Int. Ed.*, 2012, **51**, 12032–12035.
55 A. Fujishima and K. Honda, *Nature*, 1972, **238**, 37–38.
56 T. Inoue, A. Fujishima, S. Konishi and K. Honda, *Nature*, 1979, **277**, 637–638.
57 K. Zhou and Y. Li, *Angew. Chem., Int. Ed.*, 2012, **51**, 602–613.
58 Q. Xiang, J. Yu and M. Jaroniec, *Chem. Commun.*, 2011, **47**, 4532–4534.
59 H. G. Yang, C. H. Sun, S. Z. Qiao, J. Zou, G. Liu, S. C. Smith, H. M. Cheng and G. Q. Lu, *Nature*, 2008, **453**, 638–641.
60 Q. Xiang, J. Yu, W. Wang and M. Jaroniec, *Chem. Commun.*, 2011, **47**, 6906–6908.
61 J. Yu, J. Low, W. Xiao, P. Zhou and M. Jaroniec, *J. Am. Chem. Soc.*, 2014, **136**, 8839–8842.
62 L. Hammarstrom and S. H. Schiffer, *Acc. Chem. Res.*, 2009, **42**, 1859–1860.
63 H. Tada, T. Mitsui, T. Kiyonaga, T. Akita and K. Tanaka, *Nat. Mater.*, 2006, **5**, 782–786.
64 L. Amirav and A. P. Alivisatos, *J. Phys. Chem. Lett.*, 2010, **1**, 1051–1054.
65 C. Liu, J. Tang, H. M. Chen, B. Liu and P. Yang, *Nano Lett.*, 2013, **13**, 2989–2992.
66 Q. Xiang, J. Yu and M. Jaroniec, *J. Am. Chem. Soc.*, 2012, **134**, 6575–6578.
67 O. Ola and M. M. M. Valer, *Catal. Sci. Technol.*, 2014, **4**, 1631–1637.
68 W. N. Wang, W. J. An, B. Ramalingam, S. Mukherjee, D. M. Niedzwiedzki, S. Gangopadhyay and P. Biswas, *J. Am. Chem. Soc.*, 2012, **134**, 11276–11281.
69 D. Wang, T. Hisatomi, T. Takata, C. Pan, M. Katayama, J. Kubota and K. Domen, *Angew. Chem., Int. Ed.*, 2013, **52**, 11252–11256.
70 Z. Han, F. Qui, R. Eisenberg, P. L. Holland and T. D. Krauss, *Science*, 2012, **338**, 1321–1324.
71 W. J. Ong, M. M. Gui, S. P. Chai and A. R. Mohamed, *RSC Adv.*, 2013, **3**, 4505–4509.
72 M. H. Pham, C. T. Dinh, G. T. Vuong, N. D. Ta and T. O. Do, *Phys. Chem. Chem. Phys.*, 2014, **16**, 5937–5941.
73 H. Zhou, J. Guo, P. Li, T. Fan, D. Zhang and J. Ye, *Sci. Rep.*, 2013, **3**, 1667.
74 C. Wang, R. L. Thompson, J. Baltrus and C. Matranga, *J. Phys. Chem. Lett.*, 2010, **1**, 48–53.
75 X. Wang, G. Liu, L. Wang, Z. G. Chen, G. Q. Lu and H. M. Cheng, *Adv. Energy Mater.*, 2012, **2**, 42–46.